cAMP regulates plasma membrane vacuolar-type H^+-ATPase assembly and activity in blowfly salivary glands

Petra Dames*, Bernhard Zimmermann*†, Ruth Schmidt*, Julia Rein*, Martin Voss*, Bettina Schewe*, Bernd Walz*, and Otto Baumann*‡

*Institut für Biochemie und Biologie, Universität Potsdam, D-14415 Potsdam, Germany; and †Advanced Imaging Microscopy, Carl Zeiss Jena, D-07745 Jena, Germany

Communicated by Michael J. Berridge, The Babraham Institute, Cambridge, United Kingdom, January 2, 2006 (received for review August 10, 2005)

Reversible assembly of the V_0V_1 holoenzyme from V_0 and V_1 subcomplexes is a widely used mechanism for regulation of vacuolar-type H^+-ATPases (V-ATPases) in animal cells. In the blowfly (*Calliphora vicina*) salivary gland, V-ATPase is located in the apical membrane of the secretory cells and energizes the secretion of a KCl-rich saliva in response to the hormone serotonin. We have examined whether the cAMP pathway, known to be activated by serotonin, controls V-ATPase assembly and activity. Fluorescence measurements of pH changes at the luminal surface of isolated glands demonstrate that cAMP, Sp-adenosine-3′,5′-cyclic monophosphorothioate, or forskolin, similar to serotonin, cause V-ATPase-dependent luminal acidification. In addition, V-ATPase-dependent ATP hydrolysis increases upon treatment with these agents. Immunofluorescence microscopy and pelleting assays have demonstrated further that V_1 components become translocated from the cytoplasm to the apical membrane and V-ATPase holoenzymes are assembled at the apical membrane during conditions that increase intracellular cAMP. Because these actions occur without a change in cytosolic Ca^{2+}, our findings suggest that the cAMP pathway mediates the reversible assembly and activation of V-ATPase molecules at the apical membrane upon hormonal stimulus.

regulation | translocation | secretion

The vacuolar-type H^+-ATPases (V-ATPases) are multisubunit heteromeric complexes that are organized into two domains, designated V_0 and V_1 (1–4). V_0 forms a membrane-spanning proton-translocating complex; in yeast, it is composed of at least five different subunits termed a, c, c′, c″, and d, of which subunit c binds bafilomycin A_1, a specific inhibitor of V-ATPases (5–8). The V_1 sector is attached to the cytoplasmic side of the V_0 sector, consists of at least eight different subunits termed A–H, and contains catalytic and noncatalytic ATP-binding sites. V-ATPase is vital for almost every eukaryotic cell and fulfils a variety of functions. On intracellular acidic membrane systems, such as endosomes, lysosomes, and synaptic vesicles, these proton pumps are involved in protein sorting during biosynthetic and endocytotic pathways, zymogen activation, and transmitter uptake, respectively (3, 4). V-ATPase molecules in the plasma membrane of animal cells, especially on the apical plasma membrane of epithelial cells, contribute to intracellular pH homeostasis, extracellular acidification, or alkalinization, or they energize the plasma membrane for secondary transport processes (3, 4).

In some cells, V-ATPase requires a considerable amount of energy. For reasons of economy, it is thus favorable if V-ATPase activity is adapted to the physiological needs of the cell. Several regulatory mechanisms have been identified (1, 2, 4, 9). One of these is the reversible dissociation of the V_1 sector from the V_0 sector, as revealed by experiments performed in yeast, midgut epithelial cells of the tobacco hornworm *Manduca sexta*, mammalian dendritic cells, and renal epithelial cells (10–16). In the dissociated state, V-ATPase is inactive as the V_1 domain does not show ATPase activity under physiological conditions, and the V_0 domain does not translocate protons (14, 17, 18). Although reversible assembly is a widely used mechanism for V-ATPase regulation, the signaling cascades that trigger V-ATPase dissociation and reassembly remain unclear.

The blowfly salivary glands have unique morphological and physiological properties that enable the analysis of the modes of V-ATPase regulation. The secretory segments of the tubiform salivary glands consist of a single layer of uniformly differentiated epithelial cells that enclose a central lumen. The apical membrane of the secretory cells has a dense coat of V-ATPase molecules (19) and is highly enlarged by elaborate infoldings, termed canaliculi, that are lined by sheet-like microvilli (20). The activity of the proton pump is thought to establish, across the apical membrane of the secretory cells, an electrochemical gradient that is then used to drive Cl^- flux via Cl^- channels and K^+ transport by a putative K^+/nH^+ exchanger, resulting in a KCl-rich primary saliva (19). V-ATPase activity in blowfly salivary glands is under the control of serotonin (5-hydroxytryptamine, 5-HT), the hormone that elicits salivation. 5-HT stimuli induce both the assembly of V_0 and V_1 sectors to V-ATPase holoenzymes and an increase in V-ATPase-dependent hydrolytic activity (19).

The purpose of this study was to determine the second messenger system that provides the link between 5-HT receptor activation and V-ATPase regulation. It has been well established that the binding of 5-HT to its receptors on blowfly salivary gland cells induces the production of cAMP and the formation of inositol trisphosphate, the latter resulting in a rise in cytosolic Ca^{2+} concentration and an increase of Ca^{2+}-dependent Cl^- conductance (21–28). Here, we focus on the question of whether the cAMP pathway carries the information regarding 5-HT receptor activation to the V-ATPase.

Results

cAMP Induces H^+ Transport Across the Apical Membrane. It has been demonstrated previously that superfusion of glands with 10 mM cAMP leads to a monophasic change in the transepithelial potential, with an increase in lumen positivity (29–31). This finding suggested that increases in the intracellular cAMP level stimulate cation transport into the lumen of the salivary gland. To examine directly whether the cAMP pathway stimulated V-ATPase-dependent proton transport across the apical membrane, luminal pH changes were determined by ratiometric

Conflict of interest statement: No conflicts declared.

Abbreviations: Sp-cAMPS, Sp-adenosine-3′,5′-cyclic monophosphorothioate; 5-HT, 5-hydroxytryptamine; HAF, 5-*N*-hexadecanoyl-aminofluorescein; IBMX, 3-isobutyl-1-methylxanthine; PS, physiological saline; V-ATPase, vacuolar-type H^+-ATPase.

‡To whom correspondence should be addressed. E-mail: obaumann@rz.uni.potsdam.de.

www.pnas.org/cgi/doi/10.1073/pnas.0600011103

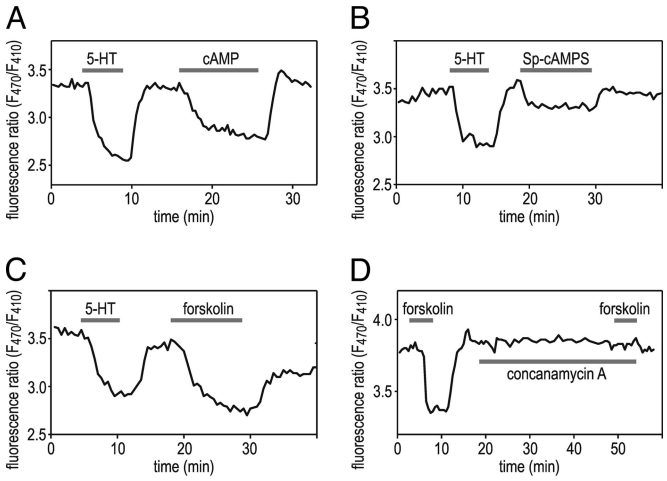

Fig. 1. Intracellular cAMP elevation causes a reversible luminal pH change that depends on V-ATPase activity. The apical membrane was labeled with pH-sensitive dye HAF, and the F_{470}/F_{410} fluorescence ratio was measured during bath application of 10 mM cAMP (*A*), 200 μM Sp-cAMPS (*B*), or 100 μM forskolin (*C* and *D*). All substances led to a reversible acidification on the luminal side of the salivary glands, as indicated by the decrease in the F_{470}/F_{410} ratio. (*D*) Preincubation with 1 μM concanamycin A abolishes the response to forskolin.

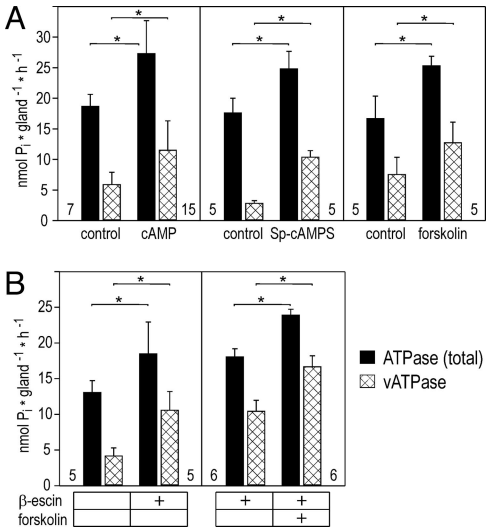

Fig. 2. Effect of cAMP, Sp-cAMP, and forskolin on total ATPase activity and bafilomycin-sensitive V-ATPase activity in homogenized salivary glands. (*A*) Preincubation of salivary glands with 10 mM cAMP, 200 μM Sp-cAMPS, or 100 μM forskolin causes a significant increase in total ATPase activity (filled bars) and V-ATPase activity (hatched bars) in tissue homogenates. (*B*) Forskolin also induces a significant increase in total ATPase activity (filled bars) and V-ATPase activity (hatched bars) after β-escin treatment of the homogenate. Values are means ± SD. Number of experiments is shown next to the base of each bar; *, $P < 0.01$.

fluorescence measurements on isolated salivary glands with 5-*N*-hexadecanoyl-aminofluorescein (HAF) injected into their lumen. The palmitoyl chain of this molecule inserts into the outer leaflet of the plasma membrane, and its pH-sensitive fluorescent moiety is then exposed on the luminal surface (32). Superfusion of the glands with a saturating concentration of 5-HT led to a reversible, monophasic luminal acidification, as indicated by the decrease in the fluorescence ratio (Fig. 1). 5-HT-induced luminal acidification was confirmed by measurements with pH-sensitive microelectrodes and was almost completely abolished by concanamycin A (J.R., B.W., and O.B., unpublished data), a specific inhibitor of V-ATPase (6). Similarly, exposure to 10 mM cAMP (Fig. 1*A*), 200 μM Sp-adenosine-3′,5′-cyclic monophosphorothioate (Sp-cAMPS) (Fig. 1*B*), a hydrolysis-resistant cAMP analogue (33), or 100 μM forskolin (Fig. 1*C*), an activator of adenylyl cyclase (34), consistently caused a decrease in the HAF fluorescence ratio. After washout of these substances, fluorescence ratio recovered to the prestimulus value within 2–3 min. The effect of forskolin was prevented by pretreatment with concanamycin A (Fig. 1*D*), demonstrating that the cAMP-dependent luminal acidification was mediated by V-ATPase.

cAMP Causes Activation of V-ATPase Activity. To determine whether cAMP stimulates V-ATPase activity, we homogenized salivary glands and measured the total ATPase activity within the homogenate and the ATP hydrolytic activity that was sensitive to bafilomycin A_1, a specific inhibitor of V-ATPase (5, 6). Treatment of salivary glands with cAMP resulted in a highly significant increase in total ATPase activity by ≈8.6 nmoles P_i per gland per hour (Fig. 2*A*). Bafilomycin-sensitive V-ATPase-dependent ATP hydrolysis was almost doubled in the presence of cAMP and accounted for the majority of the cAMP-induced rise in total ATPase activity. Similar results were obtained from salivary glands incubated with Sp-cAMPS or forskolin (Fig. 2*A*).

The cAMP pathway may act directly on V-ATPase and consequently boost its hydrolytic activity in salivary gland homogenates. Alternatively, the cAMP-dependent pathway may activate a putative K^+/nH^+ exchanger within V-ATPase-containing membrane vesicles and, thus, enhance V-ATPase hydrolytic activity indirectly. To distinguish between these possibilities, ATPase assays were performed on tissue homogenates preincubated with 50 μg/ml β-escin to permeabilize vesicular membranes. This process should have provided a shunt for a proton flux across the membrane and, thus, functionally eliminated a putative K^+/nH^+ exchanger. In the presence of β-escin, V-ATPase-dependent hydrolytic activity was increased ≈2-fold (Fig. 2*B*). This result was expected provided that vesicles could adopt two configurations stochastically during tissue homogenization, namely inside-out or right-side-out. Hence, only half of the V-ATPase molecules should have had access to ATP in the case of an intact vesicle preparation but all V-ATPase molecules should have contributed to ATP hydrolysis in the case of permeabilized vesicles. The addition of forskolin to β-escin-treated homogenate resulted in a further increase in V-ATPase hydrolytic activity (Fig. 2*B*), providing evidence that the cAMP pathway acted directly on V-ATPase.

cAMP Induces Assembly of the V-ATPase Holoenzyme. We have demonstrated previously that the majority of V-ATPase molecules in nonstimulated blowfly salivary glands are dissociated into V_0 and V_1 sectors and exposure to 5-HT induces the assembly of V_0V_1 holoenzymes (19). To examine whether the cAMP-dependent increase in V-ATPase activity is accompanied by V-ATPase assembly, salivary glands were exposed to cAMP, Sp-cAMPS, or forskolin and homogenized, and the membranes were pelleted. The relative distribution of V_0 and V_1 sector components between the pellet and the soluble fraction was then determined by Western blot analysis (Fig. 3*A*).

In control glands, 95–100% of the V_0 components subunit a and subunit d but only ≈30% and ≈43% of the V_1 components subunit A and subunit E, respectively, were recovered with the pellet (Fig. 3 *B–E*), suggesting that the majority of V_1 sectors are not incorporated into V-ATPase holoenzymes under these conditions. Upon exposure to Sp-cAMPS or forskolin, the relative amount of subunits A and E within the pellet fraction was significantly enlarged and accounted for 63–68% of the total amount of these proteins (Fig. 3 *D* and *E*), indicative of the

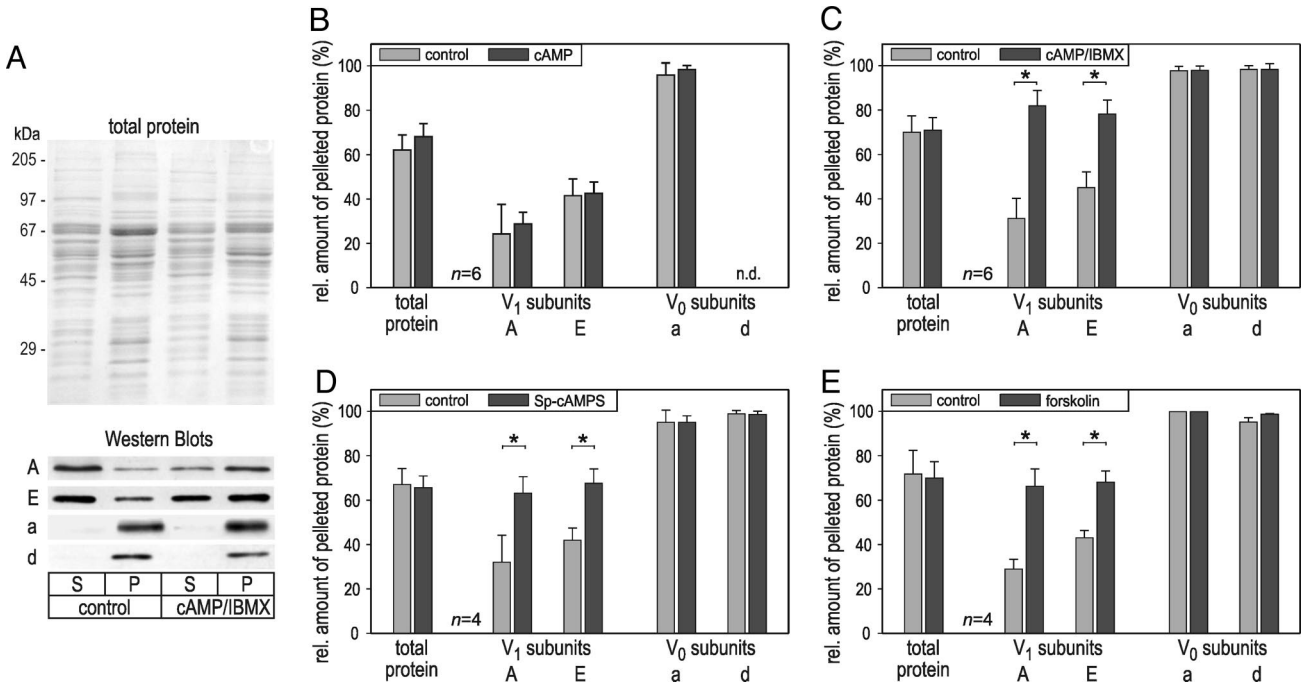

Fig. 3. Effect of cAMP, Sp-cAMP, and forskolin on the assembly state of V-ATPase. Salivary glands were exposed to 10 mM cAMP, 200 μM Sp-cAMPS, or 100 μM forskolin in PS, homogenized, and separated by ultracentrifugation into a pellet fraction (P) and a cytosolic supernatant (S). The relative distribution of V_0 (subunits a and d) and V_1 sector components (subunits A and E) between the two fractions was then probed by Western blot analysis. (*A*) Representative data of an experiment, showing the Coomassie blue-stained gel and Western blots for the various V-ATPase subunits. (*B–E*) The amount of the various V-ATPase subunits detected within the pellet relative to the total amount of the respective protein (pellet plus supernatant). Upon exposure to 200 μM Sp-cAMPS (*D*), 100 μM forskolin (*E*), or 10 mM cAMP plus 500 μM IBMX (*C*), the relative amount of V_1 sector proteins increases within the pellet; with 10 mM cAMP alone (*B*), there is no significant change ($P > 0.2$) in the distribution of these proteins. The relative distribution of V_0 sector proteins or the total amount of protein does not vary in any experiment. Data are mean ± SD. $n = 4–6$. *, $P < 0.01$; n.d., not determined.

recruitment of V_1 sectors to the membrane and the assembly of V-ATPase holoenzymes. In the case of cAMP, however, we did not observe a significant change in the relative amount of subunits A and E within the pellet fraction (Fig. 3*B*). Because V-ATPase holoenzyme assembly is a reversible process (10–14), we reasoned that this discrepancy in results might be caused by cAMP hydrolysis and disassembly of V-ATPase holoenzymes during the course of the experiment, from tissue homogenization until the end of ultracentrifugation; forskolin, in contrast, may continuously activate adenylyl cyclase and thus provide a high concentration of cAMP during the entire experiment, and Sp-cAMPS is resistant to hydrolysis (33). To examine this possibility, solutions were supplemented with 3-isobutyl-1-methylxanthine (IBMX), an inhibitor of phosphodiesterase. Under these conditions, cAMP led to an enrichment of subunits A and E within the pellet fraction (Fig. 3*C*), supporting the above hypothesis. We thus conclude that the assembly status of V-ATPase is under the control of cAMP, with increases in cAMP concentration leading to an assembly of holoenzymes.

cAMP Induces a Recruitment of V-ATPase Subunits to the Apical Membrane. To determine whether cAMP-induced assembly of V-ATPase is accompanied by a translocation of its subcomplexes, cryosections were labeled with antibodies against subunit d (V_0 domain) and subunit B (V_1 domain). In control cells, V_0 component subunit d was highly concentrated at the apical membrane (Fig. 4 *A* and *B*) that was identified by intense labeling for actin (Fig. 4 *E* and *F*) (19, 26). In addition, numerous vesicular structures scattered throughout the cell were stained for subunit d, but these structures contained only a minor fraction (10–20%) of the total staining intensity for subunit d. V_1 component subunit B, in contrast, appeared to be homogeneously distributed in the cytoplasm of nonstimulated cells, being only slightly enriched on the apical membrane (Fig. 4 *C* and *G*). In cAMP-treated (data not shown) or forskolin-treated glands (Fig. 4 *B*, *D*, *F*, and *H*), cytoplasmic staining for subunit B was highly reduced and the apical membrane was highlighted by intense labeling for subunit B and subunit d, suggesting that V_1 subcomplexes translocated from the cytoplasm to the apical membrane. Moreover, the number of vesicular structures with V_0 staining appeared to be reduced in cAMP- or forkolin-treated cells (Fig. 4*B*), indicating that some of these membranes became integrated into the apical membrane upon stimulation. Notably, most of these vesicular structures were not enriched for subunit B even in forskolin-treated cells (Fig. 4 *D* and *H Insets*), suggesting that they contained only V_0 domains.

A Rise in Cytosolic Ca^{2+} Is Not Required for V-ATPase Stimulation. Because cAMP is reported to affect intracellular Ca^{2+} signaling and may even induce Ca^{2+} mobilization in various cell types (35, 36), we have determined whether effectors on the cAMP pathway cause a rise in cytosolic Ca^{2+} in blowfly salivary glands. Fig. 5 shows that cAMP did not elevate cytosolic Ca^{2+}, whereas a subsequent stimulus with 5-HT evoked a rapid Ca^{2+} response. Identical results were obtained with Sp-cAMPS and forskolin (data not shown). These results demonstrate that cAMP-induced assembly and enhancement of V-ATPase hydrolytic activity occur without cytosolic Ca^{2+} elevation.

Discussion

Reversible dissociation of the V-ATPase complex into its component V_0 and V_1 domains is an important mechanism for regulation of V-ATPase activity in various systems. In yeast, in which this process has been studied most comprehensively to

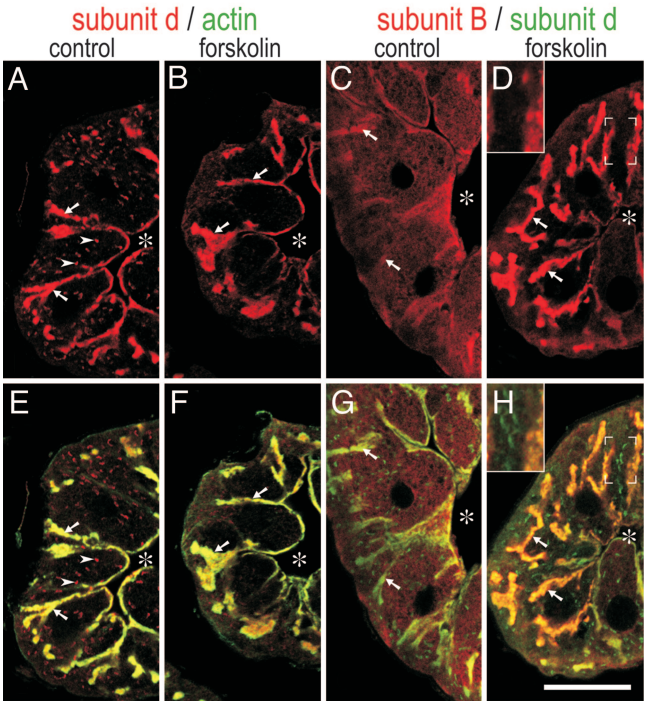

Fig. 4. Distribution of V_0 and V_1 components in control and forskolin-treated (100 μM) salivary glands. Cross sections through salivary glands were double-labeled with antibodies against V_0 subunit d (red in *A*, *B*, *E*, and *F*) and actin (green in *E* and *F*) or antibodies against V_1 subunit B (red in *C*, *D*, *G*, and *H*) and V_0 subunit d (green in *G* and *H*). (*E* and *F*). The apical membrane with its deep infoldings (= canaliculi; arrows) is revealed by intense labeling for actin. Asterisks indicate the lumen of the gland. (*A* and *B*) Subunit d is highly enriched on the apical membrane in control and forskolin-treated glands. (*C*, *D*, *G*, and *H*) Subunit B is concentrated at the apical membrane only in the forskolin-treated gland. Vesicular staining for subunit d (arrowheads) is frequent in the control (*A*) and reduced in forskolin-treated cells (*B*). These structures are stained for subunit d but not subunit B (*D* and *H Insets*). (Scale bar, 20 μm.)

date, V-ATPase dissociation occurs upon glucose deprivation and does not involve any conventional signaling pathways that are known to be activated by glucose depletion, such as the protein kinase C pathway and the Ras–cAMP pathway (10, 13, 37). Instead, recent studies suggest that the glycolytic enzyme aldolase may act as a glucose sensor and mediate V-ATPase assembly by binding simultaneously to V_0 and V_1 sector proteins (38). In midgut epithelial cells of *M. sexta* larvae, another model system for analyzing the structure and function of V-ATPase, reversible V-ATPase dissociation occurs during starvation or

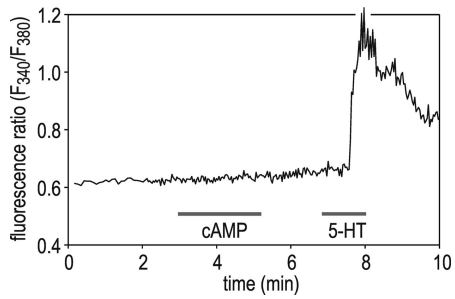

Fig. 5. Effect of cAMP on cytoplasmic [Ca^{2+}] in Fura-2-loaded salivary glands. Bath application of 10 mM cAMP has no obvious effect on the cytosolic Ca^{2+} concentration, whereas 30 nM 5-HT causes a transient Ca^{2+} elevation.

moulting (11, 12). However, the signaling pathways that induce and regulate V-ATPase assembly/disassembly are unclear.

We have recently shown that the blowfly salivary gland represents another example of V-ATPase regulation via a reversible assembly process (19). V-ATPase assembly occurs in this system shortly after receiving a hormonal signal and this organ is accessible to various biochemical and physiological techniques, including pH measurements with fluorescent dyes in distinct compartments. Thus, the blowfly salivary gland may serve as a valuable model for analyzing the mechanisms involved in this mode of V-ATPase regulation. Upon a stimulus with 5-HT (the hormone that regulates salivation of the blowfly), the amount of cytosolic V_1 components decreases, whereas the amount of membrane-associated V_1 components and the hydrolytic activity of V-ATPases increase in parallel (19). The findings reported here show that the cAMP pathway provides the link between activated 5-HT receptor molecules on the basolateral side of the epithelial cells and the reversible assembly and activation of V-ATPase molecules on the apical membrane domain.

All pharmacological interventions that lead to an elevation in the intracellular cAMP concentration fully mimic the effects of 5-HT with respect to the assembly status and the hydrolytic and proton-pumping activity of V-ATPase. First, pH measurements at the luminal surface with the fluorescent membrane-integrating dye HAF have demonstrated a reversible acidification of the luminal space in response to cAMP, Sp-cAMPS, or forskolin. Inhibition by concanamycin A has confirmed that the cAMP-induced luminal acidification was caused by H^+ transport across the apical membrane by means of V-ATPase. Second, these substances consistently lead to an increase of ≈2-fold in V-ATPase-dependent ATP hydrolysis and a parallel 2-fold increase in the amount of membrane-associated V_1 components, indicative of the assembly of V_0V_1 holoenzymes. Finally, cAMP or forskolin treatment resulted in a translocation of V_1 component subunit B from the cytoplasm to the apical membrane, supporting the conclusion that V_0V_1 holoenzymes become assembled on the apical membrane in a cAMP-dependent manner.

The results of our pelleting assays with cAMP alone, in particular, the lack of an increase in the amount of membrane-associated V_1 components under these conditions, may appear puzzling and to contradict the above notion of a cAMP-induced V-ATPase assembly. However, we present evidence suggesting this result reflects the hydrolytic activity of phosphodiesterases during the pelleting assay and the reversibility of V-ATPase assembly. In the presence of IBMX, an inhibitor of phosphodiesterases, cAMP led to an increase in the amount of membrane-associated V_1 components, similar to forskolin or the hydrolysis-resistant cAMP analogue Sp-cAMPS. Moreover, immunofluorescence microscopy has demonstrated a cAMP-induced translocation of subunit B from the cytoplasm to the apical membrane, indicative of V-ATPase assembly in the intact salivary gland.

V-ATPase is not restricted to the apical membrane but can also be detected on intracellular acidic organelles (3, 4). Indeed, immunofluorescence microscopy has visualized intracellular vesicular structures with staining for subunit d. However, most of these structures lacked staining for V_1 subunit B and may thus represent an intracellular reserve pool of V_0 sectors rather than acidic organelles that require functional V-ATPase. Support for this interpretation was provided by our finding that vesicular V_0 staining decreased upon forskolin treatment, suggesting that these structures are translocated and integrated into the apical membrane in a cAMP-dependent manner. Notably, these intracellular V_0-containing structures were short of subunit B staining even upon forskolin treatment, although the cytoplasmic pool of subunit B was

highly reduced. V_1 components may thus preferentially associate with V_0 sectors in the apical membrane.

Regulation via the cAMP pathway seems to be a widespread mechanism for the control of V-ATPase activity. Evidence has been presented that cAMP activates an apical V-ATPase in *Drosophila* Malpighian tubules (39, 40) and the gill epithelium of the crab *Eriocheir sinensis* (41). Moreover, pH regulation in rat epididymis is mediated by V-ATPase and regulated by a bicarbonate-activated soluble adenylyl cyclase (42). In all of these examples, however, the mode of V-ATPase regulation involves either the cycling of V-ATPase molecules between an intracellular vesicular pool and the plasma membrane (42) or is still undisclosed. Thus, we have identified the second messenger that controls reversible V-ATPase assembly in an animal cell. For the downstream mechanisms activated by cAMP and leading to V-ATPase assembly and activation, two scenarios might be considered *a priori*: (*i*) activation of protein kinase A and phosphorylation of V-ATPase subunits or V-ATPase-interacting proteins; and (*ii*) activation of EPAC (exchange protein directly activated by cAMP) (43, 44), followed by EPAC-catalyzed exchange of GDP for GTP on Rap-like small G proteins that may then either bind to V-ATPase subunits or interacting proteins or activate downstream protein kinases (45).

In addition to the increase in cAMP concentration, 5-HT induces, via the phospholipase C/inositol trisphosphate pathway, a rise in cytosolic Ca^{2+} concentration in the blowfly salivary gland (22–24, 27). This finding raises, in principle, the possibility that the latter pathway contributes to the regulation of V-ATPase assembly and/or activity *in vivo*. Because our pharmacological interventions that led to an elevation of intracellular cAMP concentration occur without a change in cytosolic Ca^{2+} concentration, our findings at least demonstrate that the cAMP pathway is sufficient for V-ATPase regulation. We cannot exclude, however, that the phospholipase C/inositol trisphosphate/Ca^{2+} pathway plays a modulatory role in regulating V-ATPase assembly and/or activity.

Materials and Methods

Animals and Preparation. Blowflies (*Calliphora vicina*) were reared at the Universität Potsdam. One to four weeks after the eclosion of the flies, the abdominal portions of their salivary glands were dissected and used for experiments. Physiological saline (PS) contained 128 mM NaCl, 10 mM KCl, 2 mM $CaCl_2$, 2 mM $MgCl_2$, 2.7 mM Na-Glu, 2.7 mM malic acid, 10 mM Glc, and 10 mM Tris·HCl (pH 7.2).

Reagents. Antisera against the following proteins were used: bovine V-ATPase subunits A and E (46), *Culex quinquefasciatus* V-ATPase subunit B (47), and *M. sexta* V-ATPase subunits a and d (provided by H. Wieczorek, Universität Osnabrück, Osnabrück, Germany). The cross-reactivity of these antisera with the corresponding *Calliphora* V-ATPase subunits has been demonstrated (19). Monoclonal anti-actin (clone C4) was purchased from MP Biomedicals (Irvine, CA). Horseradish peroxidase-conjugated secondary antibodies were obtained from American Qualex (La Mirada, CA), and fluorophore-tagged secondary antibodies were from Dianova (Hamburg, Germany) or Invitrogen. Fura-2 acetoxymethyl ester and HAF (20 mM stock solution in DMSO) were obtained from Invitrogen. The following inhibitors and stimuli were used at the concentrations indicated, unless otherwise stated: 5-HT (30–100 nM) and concanamycin A (1 μM) were from Sigma. cAMP (10 mM) and IBMX (500 μM) were from Serva. Sp-cAMPS (200 μM) was from Tocris Bioscience (Avonmouth, U.K.). Forskolin (100 μM) was from Axxora (Grünberg, Germany).

Microfluorometric Measurements of Luminal pH. For monitoring pH changes at the luminal surface of the secretory cells, we adapted a microfluorometric method that was previously used on guinea pig colonic epithelium (32). The fatty acyl chain of this dye integrates into the outer leaflet of the plasma membrane, and its pH-sensitive fluorescent moiety faces then the extracellular space (32). Salivary glands were attached to the Cell-Tak-coated (BD Biosciences, San Jose, CA) surface of a glass-bottom perfusion chamber that was then placed on a Zeiss Axiovert 135 inverted microscope. A microelectrode filled with 30 μM HAF in PS was inserted through the open end of the tubule into the lumen of the salivary gland, and HAF solution was pressure-injected into the lumen by using a pneumatic picopump (PV820; World Precision Instruments, Sarasota, FL). Confocal imaging has confirmed that HAF inserts into the apical membrane of the secretory cells and remains restricted to the luminal surface (J.R., B.W., and O.B., unpublished data). HAF fluorescence was alternately excited through a Zeiss ×20 Fluar, 0.75 numerical aperture objective at wavelengths 410 and 470 nm provided by a xenon arc lamp and a VisiChrome monochromator unit (Visitron Systems, Puchheim, Germany). After passage through a 515 long-pass filter, the emitted light was recorded with a cooled charge-coupled device camera (CoolSnap HQ; Photometrics, Tucson, AZ), digitized, and transferred to a personal computer for offline calculation of the fluorescence ratio at 470- and 410-nm excitation (F_{470}/F_{410} ratio) with the imaging software METAFLUOR 6.1 (Universal Imaging, Downingtown, PA). A decrease in F_{470}/F_{410} ratio reflects an acidification, and an increase in F_{470}/F_{410} ratio represents an alkalization (32).

V-ATPase Activity Assays. Glands were isolated and divided into two pools; the experimental group was incubated for 3 min (5-HT), 5–6 min (cAMP; forskolin), or 10–12 min (Sp-cAMPS) with the respective agent diluted in PS. Subsequently, the glands were homogenized on ice in buffer A (0.3 M sucrose/0.1 mM EGTA/0.1% β-mercaptoethanol/0.1 M imidazol, pH 7.2), supplemented with a mixture of protease inhibitors (Sigma) and the respective test reagent (0.1 mM cAMP, 200 μM Sp-cAMPS, or 100 μM forskolin). Okadaic acid (1 μM) was added as a protein phosphatase inhibitor to preserve the phosphorylation status of proteins within the homogenate in case cAMP led to V-ATPase phosphorylation. The control group was bathed for an equal amount of time in PS and then homogenized in buffer A supplemented with protease inhibitors. All further conditions, including the determination of P_i as a phosphomolybdate complex (48), were as described (19). In the case of β-escin treatment, the homogenate was preincubated for 10 min with 50 μg/ml β-escin before starting the hydrolytic reaction by the addition of ATP.

Pelleting Assays. For assessing the assembly state of V-ATPase, salivary glands were incubated in PS containing the respective pharmacological agent, as described above. Control glands were then homogenized on ice in extraction buffer (70 mM sucrose/50 mM KCl/20 mM DTT/50 mM Tris, pH 7.2/protease inhibitor mixture), whereas experimental glands were homogenized in extraction buffer supplemented with the respective reagent (0.1 mM cAMP, 200 μM Sp-cAMPS, or 100 μM forskolin) and 1 μM okadaic acid. The homogenates were then centrifuged for 30 min at 150,000 × g at 4°C to separate the membranes from the cytosolic fraction. Samples were resuspended in reducing sample buffer (Carl Roth, Karlsruhe, Germany) and heated for 5 min to 60°C. SDS/PAGE, Western blotting, immunostaining, and densitometric analysis of immunolabeling were performed as described (19).

Immunofluorescence Staining of V-ATPase and Confocal Microscopy. Control and forskolin-treated glands were fixed, cryosectioned, and labeled as described (19), except that sections were pre-

treated for 3 min with 1% SDS in PBS to increase accessibility of epitopes and blocked for 15 min with 3% dry milk, 1% goat serum, 0.8% BSA, and 0.5% Triton X-100 in PBS. Fluorescence images were recorded with a Zeiss LSM 510 confocal laser scanning microscope and analyzed with METAMORPH (Universal Imaging).

Other Methods. Fluorescence analyses of cytosolic Ca^{2+} changes were performed on Fura-2-loaded glands as described (27). Data were tested for significance with Student's *t* test; only results with $P < 0.01$ were considered statistically significant.

We thank Angela Hubig and Stefanie Herold for excellent technical assistance; Helmut Wieczorek for generously providing reagents and comments on the manuscript; and Irene Schulz (Universität des Saarlandes, Saarbrücken, Germany) and Sarjeet S. Gill (University of California, Riverside) for providing antibodies. This work was supported by Deutsche Forschungsgemeinschaft Grants Wa463/9-3 and GRK837.

1. Stevens, T. H. & Forgac, M. (1997) *Annu. Rev. Cell Dev. Biol.* **13,** 779–808.
2. Forgac, M. (1999) *J. Biol. Chem.* **274,** 12951–12954.
3. Nelson, N. & Harvey, W. R. (1999) *Physiol. Rev.* **79,** 361–385.
4. Nishi, T. & Forgac, M. (2002) *Nat. Rev. Mol. Cell. Biol.* **3,** 94–103.
5. Bowman, E. J., Siebers, A. & Altendorf, K. (1988) *Proc. Natl. Acad. Sci. USA* **85,** 7972–7976.
6. Dröse, S. & Altendorf, K. (1997) *J. Exp. Biol.* **200,** 1–8.
7. Huss, M., Ingenhorst, G., Konig, S., Gassel, M., Drose, S., Zeeck, A., Altendorf, K. & Wieczorek, H. (2002) *J. Biol. Chem.* **277,** 40544–40548.
8. Bowman, B. J. & Bowman, E. J. (2002) *J. Biol. Chem.* **277,** 3965–3972.
9. Wieczorek, H., Brown, D., Grinstein, S., Ehrenfeld, J. & Harvey, W. R. (1999) *BioEssays* **21,** 637–648.
10. Kane, P. M. (1995) *J. Biol. Chem.* **270,** 17025–17032.
11. Sumner, J. P., Dow, J. A., Earley, F. G., Klein, U., Jager, D. & Wieczorek, H. (1995) *J. Biol. Chem.* **270,** 5649–5653.
12. Wieczorek, H., Gruber, G., Harvey, W. R., Huss, M., Merzendorfer, H. & Zeiske, W. (2000) *J. Exp. Biol.* **203,** 127–135.
13. Kane, P. M. (2000) *FEBS Lett.* **469,** 137–141.
14. Kane, P. M. & Smardon, A. M. (2003) *J. Bioenerg. Biomembr.* **35,** 313–321.
15. Trombetta, E. S., Ebersold, M., Garrett, W., Pypaert, M. & Mellman, I. (2003) *Science* **299,** 1400–1403.
16. Sautin, Y. Y., Lu, M., Gaugler, A., Zhang, L. & Gluck, S. L. (2005) *Mol. Cell. Biol.* **25,** 575–589.
17. Zhang, J., Myers, M. & Forgac, M. (1992) *J. Biol. Chem.* **267,** 9773–9778.
18. Gräf, R., Harvey, W. R. & Wieczorek, H. (1996) *J. Biol. Chem.* **271,** 20908–20913.
19. Zimmermann, B., Dames, P., Walz, B. & Baumann, O. (2003) *J. Exp. Biol.* **206,** 1867–1876.
20. Oschman, J. L. & Berridge, M. J. (1970) *Tissue Cell* **2,** 281–310.
21. Heslop, J. P. & Berridge, M. J. (1980) *Biochem. J.* **192,** 247–255.
22. Berridge, M. J. & Heslop, J. P. (1981) *Br. J. Pharmacol.* **73,** 729–738.
23. Fain, J. N. & Berridge, M. J. (1979) *Biochem. J.* **178,** 45–58.
24. Berridge, M. J. (1983) *Biochem J.* **212,** 849–858.
25. Berridge, M. J., Dawson, R. M. C., Downes, C. P., Heslop, J. P. & Irvine, R. F. (1983) *Biochem. J.* **212,** 473–482.
26. Zimmermann, B. (2000) *Cell Calcium* **27,** 297–307.
27. Zimmermann, B. & Walz, B. (1997) *J. Physiol. (London)* **500,** 17–28.
28. Berridge, M. J., Lindley, B. D. & Prince, W. T. (1975) *J. Physiol. (London)* **244,** 549–567.
29. Prince, W. T. & Berridge, M. J. (1972) *J. Exp. Biol.* **56,** 323–333.
30. Berridge, M. J. & Prince, W. T. (1972) *J. Exp. Biol.* **56,** 139–153.
31. Berridge, M. J. & Prince, W. T. (1972) *Adv. Insect Physiol.* **9**, 1–49.
32. Genz, A.-K., von Engelhardt, W. & Busche, R. (1999) *J. Physiol. (London)* **517,** 507–519.
33. Schaap, P., Ments-Cohen, M., Soede, R. D., Brandt, R., Firtel, R. A., Dostmann, W., Genieser, H. G., Jastorff, B. & van Haastert, P. J. (1993) *J. Biol. Chem.* **268,** 6323–6331.
34. Seamon, K. B., Padgett, W. & Daly, J. W. (1981) *Proc. Natl. Acad. Sci. USA* **78,** 3363–3367.
35. Bruce, J. I., Straub, S. V. & Yule, D. I. (2003) *Cell Calcium* **34,** 431–444.
36. Schmidt, M., Evellin, S., Weernink, P. A., von Dorp, F., Rehmann, H., Lomasney, J. W. & Jakobs, K. H. (2001) *Nat. Cell Biol.* **3,** 1020–1024.
37. Parra, K. J. & Kane, P. M. (1998) *Mol. Cell. Biol.* **18,** 7064–7074.
38. Lu, M., Sautin, Y. Y., Holliday, L. S. & Gluck, S. L. (2004) *J. Biol. Chem.* **279,** 8732–8739.
39. O'Donnell, M. J., Dow, J. A., Huesmann, G. R., Tublitz, N. J. & Maddrell, S. H. (1996) *J. Exp. Biol.* **199,** 1163–1175.
40. Coast, G. M., Webster, S. G., Schegg, K. M., Tobe, S. S. & Schooley, D. A. (2001) *J. Exp. Biol.* **204,** 1795–1804.
41. Onken, H., Schobel, A., Kraft, J. & Putzenlechner, M. (2000) *J. Exp. Biol.* **203,** 1373–1381.
42. Pastor-Soler, N., Beaulieu, V., Litvin, T. N., Da Silva, N., Chen, Y., Brown, D., Buck, J., Levin, L. R. & Breton, S. (2003) *J. Biol. Chem.* **278,** 49523–49529.
43. De Rooij, J., Zwartkruis, F. J., Verheijen, M. H., Cool, R. H., Nijman, S. M., Wittinghofer, A. & Bos, J. L. (1998) *Nature* **396,** 474–477.
44. Bos, J. L. (2003) *Nat. Rev. Mol. Cell. Biol.* **4,** 733–738.
45. Hattori, M. & Minato, N. (2003) *J. Biochem.* **134,** 479–484.
46. Roussa, E., Thevenod, F., Sabolic, I., Herak-Kramberger, C. M., Nastainczyk, W., Bock, R. & Schulz, I. (1998) *J. Histochem. Cytochem.* **46,** 91–100.
47. Filippova, M., Ross, L. S. & Gill, S. S. (1998) *Insect Mol. Biol.* **7,** 223–232.
48. Bonting, S. L., Simon, K. A. & Hawkins, N. M. (1961) *Arch. Biochem. Biophys.* **95,** 416–423.